



Design of automated adaptive controller for mean arterial pressure in hypotensive situations using a vasopressor drug

Marcelo Saraiva Coelho^{1,2} · Samuel Justino da Silva¹ · Terigi Augusto Scardovelli¹ ·
Silvia Regina Matos da Silva Boschi¹ · Silvia Cristina Martini Rodrigues¹ · Alessandro Pereira da Silva¹

Received: 12 December 2021 / Accepted: 9 April 2022 / Published online: 19 April 2022
© Sociedade Brasileira de Engenharia Biomedica 2022

Abstract

Purpose Patients with hypotension in emergency clinical situations require the administration of vasopressor drugs for a fast and correct return of the mean arterial pressure, done by either manual or automated administration which can be done by either manual or automated administration. The proportional-integral-derivative (PID) algorithm has been used for several years as one of the most understandable and easily implemented automatic control techniques. However, in situations where there is variability in the parameters of the process you want to control, as in the case of the mean arterial pressure (MAP) response in patients undergoing vasopressor infusion, the automatic control system can become challenging. This paper describes the development of a controller, considering the real-time identification of several types of patients.

Methods The MAP response for phenylephrine (PHP) drug infusion and the controller were modeled by the MATLAB/Simulink computational tool and embedded each one on simple hardware platforms based on the low-cost microcontroller. The controller was designed considering a time for patient identification, allowing its adjustment according to the patient. To validate the feasibility of the controller, tests were conducted verifying the performance both in a computer simulation environment and in hardware-in-the-loop (HIL) simulation. In these tests, three tuning methods were used for control, based on the consolidated methods developed by Ziegler-Nichols and Skogestad.

Results The results obtained show that the patient identification occurs in 200 s. The MAP control was obtained with a steady-state error of less than 0.31 mmHg, settling time with a maximum of 240.5 s, and peak overshoot of desired MAP value on the order of 5.5 mmHg in its worst case, considering all tuning methods.

Conclusion The developed control system can identify the patient's response type. The results obtained indicated that the controller demonstrated to be suitable for low peak overshoot and steady-state error values, allowing a smoother MAP control.

Keywords Biomedical control system · Adaptive control scheme · Embedded PID controller · Mean arterial pressure regulation · Hypotension

✉ Marcelo Saraiva Coelho
mcoelho@ifsp.edu.br

Samuel Justino da Silva
samuel.silva@fecaf.com.br

Terigi Augusto Scardovelli
terigiscardovelli@umc.br

Silvia Regina Matos da Silva Boschi
boschi@umc.br

Silvia Cristina Martini Rodrigues
silviac@umc.br

Alessandro Pereira da Silva
alessandrops@umc.br

¹ Technology Research Center, University of Mogi das Cruzes, (UMC), Mogi das Cruzes, SP, Brazil. Av. Dr. Cândido Xavier de Almeida e Souza, 200, Mogi das Cruzes, SP CEP 08780-911, Brazil

² Federal Institute of Education Science and Technology of Sao Paulo (IFSP), Cubatão, SP, Brazil. Rua Maria Cristina, 50, Cubatão, SP CEP 11533-160, Brazil

Introduction

Hypotension during non-cardiac surgery is associated with increased mortality from complications in postoperative periods (Monk et al. 2015). In these cases, the risk of organ injuries increases when the MAP remains below 80 mmHg for more than 10 min or below 70 mmHg for less than 10 min (Wesselink et al. 2018).

Hypotension is often one of the complications in cesarean surgeries with spinal anesthesia (das Neves et al. 2010). The risk of postoperative acute kidney injury increase when intraoperative MAP is less than 60 mmHg for more than 20 min and less than 55 mmHg for more than 10 min (Sun et al. 2015). In vascular surgery for elderly patients, intraoperative hypotension is defined as a 40% reduction in pre inductive MAP for more than 30 min and is associated with postoperative myocardial injury (Van Waes et al. 2016). Intraoperative hypotension increases the risk of postoperative cerebrovascular accidents, especially when MAP values decrease by more than 30% of baseline MAP. The MAP value to initiate the use of vasopressors is set at 65 mmHg. However, it is possible to consider values slightly higher than this, especially when dealing with patients previously diagnosed with hypertension (Rhodes et al. 2017). The use of norepinephrine (NE), epinephrine (EPP), ephedrine (EPD), and phenylephrine (PHP)

as a vasopressor drug is widely used to control hypotension, especially in surgeries that use spinal anesthesia (Lee et al. 2017). Although studies on MAP control began a long time ago, the current standard for guide vasopressor infusion is manual titration, in which the professional responsible for patient care set infusion rates in response to MAP variations (Rinehart et al. 2021). In part, this can be explained by the challenge to control MAP, when a large variability in parameters related to the pharmacological response of patients on the administration of vasopressors, e.g., NE and PHP. Researches have studied a wide range of control models as a proposals for solutions, including proportional-integral (PI) control and its alternatives, adaptive control, rule-based control, and intelligent control (Sathish and Nachiappan 2019). Table 1 presents the main articles about MAP control in hypotensive conditions (Davoud et al. 2020; Fung et al. 2004; Huang and Roy 1998; Kashiwara et al. 2004; Kashiwara 2018; Ngan Kee et al. 2007, 2012, 2017; Rinehart et al. 2017, 2018; Soltesz et al. 2017; Tasoujian et al. 2019, 2020).

In contrast with systems of MAP control for hypertension, in which the vasodilator drug sodium nitroprusside (SNP) presents a model already consolidated and referenced by (Slate and Sheppard 1982), the mathematical models suggested for vasopressor drugs response are not widely available. Among these models, those developed by Rinehart et al. (2011) and

Table 1 MAP hypotension controllers review

Article's author	Year	Drug	Control strategy	Control test		
				Computer simulation	Animal studies	Human studies
Davoud et al	2020	Norepinephrine	ADP	x		
Tasoujian et al	2020	Phenylephrine	PID LPV-MMSRCKF	x		
Kashiwara	2018	Norepinephrine	DCNN		x	
Tasoujian et al	2019	Phenylephrine	PID-IMC	x		
Rinehart et al	2018	Norepinephrine	PID-Rules		x	
Rinehart et al	2017	Norepinephrine	PID-Rules		x	
Soltesz et al	2017	Cocktail	PI; PID Filter		x	
Ngan Kee et al	2017	Phenylephrine Nor-epinephrine	ON-OFF			x
Luspay et al	2015	Phenylephrine	PID LPV-MMEKF	x		
Wassar et al	2014	Phenylephrine	PI-AW	x	x	
Ngan Kee et al	2012	Phenylephrine	ON-OFF			x
Ngan Kee et al	2007	Phenylephrine	ON-OFF			x
Fung et al	2004	Phenylephrine	PID-MPC	x		
Kashiwara et al	2004	Norepinephrine	PID; MPC; APC _{NN} ; APC _{NN-PID} ; PID FUZZY	x	x	
Huang and Roy	1998	Phenylephrine	Fuzzy	x		

ADP adaptive dynamic programming, LPV-MMSRCKF linear parameter varying–multiple model square root cubature Kalman filter for estimation, DCNN deep convolutional neural networks, PID-IMC proportional-integral-derivative internal model control, PID-Rules proportional-integral-derivative with rules-based decision engine, ON-OFF two-position, LPV-MMEKF multiple-model extended Kalman filter structure for estimation, PID-AW proportional-integral-derivative anti-windup, MPC model predictive control, APC_{NN} adaptive predictive control based on neural network, APC_{NN-PID} combined control of APC_{NN} and PID, PID-FUZZY proportional-integral-derivative control based on fuzzy logic

Luspay and Grigoriadis (2015) can be highlighted. We used the last one as the basis for patient simulation.

This paper describes the development and testing of an adaptive controller embedded in simple hardware considering the variabilities in the MAP response of patients in relation to PHP infusion, providing adaptability in the automatic MAP control system for different types of patients. The control type is composed of a PID controller, whose gain parameters are estimated from the identification system of the patient’s characteristics, using a recursive polynomial model estimator, autoregressive with exogenous input (ARX) using estimation algorithm by recursive least squares with forgetting factor.

Methods

Patient model

The mathematical model for the patient simulation presented in Fig. 1 is derived from the studies of Luspay and Grigoriadis (2015) and Wassar et al. (2014), considering the existence of a regressive nonlinear relationship between PHP injection defined as $u(t)$ and MAP response as $MAP(t)$ obtained in animal trials.

Because variations were observed between animals, as well as variability during the infusion time, it was possible to verify that for step variation of PHP injection, the MAP response variation can be represented by a simplified first-order transfer function with time delay, as shown in Eq. (1).

$$\frac{\Delta P(s)}{I(s)} = \frac{K}{\tau s + 1} e^{-Ts} \tag{1}$$

where.

ΔP = Mean arterial pressure variation (mmHg);

I = PHP infusion rate (mL/h);

K = Patient sensitivity (mmHg.h.mL⁻¹);

τ = Time constant of drug application representing drug absorption, distribution and metabolism (s);

T = Delay time of the injection line (s).

The main transfer function is influenced by changes in its parameters during the time and intensity of the drug injection rate, thus allowing the simulation of the physiological response of different types of patients. The equations for the parameter variations are shown in (2) to (5).

$$G_T(s) = \begin{cases} \sigma [T_{\min}, T_{\max}] \left\{ \frac{b_{T1}s + b_{T0}}{a_{T2}s^2 + a_{T1}s + a_{T0}} \right\} I(s) \rightarrow t \geq t_0 \\ 0 \rightarrow otherwise \end{cases} \tag{2}$$

$$G_K(s) = K_0 \times e^{\left[-K_1 \times I(s) \times \frac{1}{a_{K0}s+1} \right]} \tag{3}$$

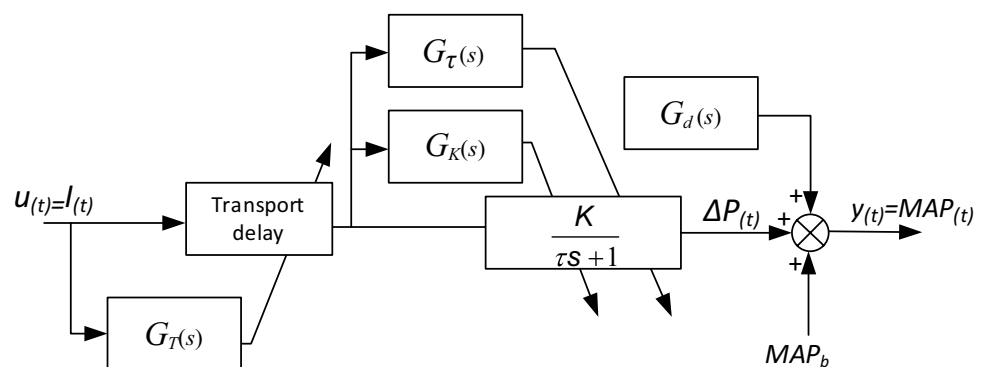
$$G_\tau(s) = \frac{b_{\tau 0}}{s} \times I(s) \tag{4}$$

$$G_d(s) = \frac{b_d}{a_d s + 1} \tag{5}$$

where I is the PHP infusion rate, T is the delay time of the injection, σ is a saturation function to limit its value between the bounds of T_{\min} and T_{\max} , K_0 is the nominal sensitivity in relation to PHP, K_1 is the dynamic sensitivity (mmHg/ml h⁻¹), a_{K0} is the coefficient of the sensitivity transfer function fixed in 550, $b_{\tau 0}$ is the integration coefficient of the time constant variation, $a_d=40$ and $b_d=5$ are coefficients of stochastic activity and the patient’s breathing effects function and $a_{T0}=1$, $a_{T1}=10$, $a_{T2}=10$, $b_{T0}=1$, and $b_{T1}=100$ are delay time coefficients of function. During simulation and testing, some parameters were maintained with constant values, such as $a_{K0}=550$, $a_d=40$, $b_d=5$, $a_{T0}=1$, $a_{T1}=10$, $a_{T2}=10$, $b_{T0}=1$, and $b_{T1}=100$.

The $G_T(s)$ block is responsible for the random variation of the delay time at the drug injection. The delay time has a short peak period during the initial injection of the drug, a value that gradually decreases with other injections. The $G_K(s)$ block is responsible for the dynamic variation of the patient’s sensitivity and shows that patients gradually lose sensitivity to a given vasoactive drug through their subsequent injection. The $G_\tau(s)$ block is responsible for the

Fig. 1 Patient simulation model



dynamic variation of the time constant in response to the injection of the drug. The time constant increases slowly from an initial value, according to the amount of injection of the drug. The $G_d(s)$ block represents stochastic activity and the patient's breathing effects. The simulation allows the variation of all parameters between their limits. However, for this study, 10 types of patients were defined as presented in Table 2 (Coelho et al. 2020).

System identification

System identification is the technique for developing mathematical models of a dynamic system based on observed input and output data. It is a statistical method used to estimate unknown model parameters, i.e., the coefficients in the differential equation. The model identification approach is named Identification for Control (I4C) if the model applicability is valid under certain boundary conditions (De Carvalho et al. 2021).

A decisive step in the identification procedure is the appropriate model type selection (Aguirre 2015). The representation of the general linear model can be considered as follows:

$$y(k) = \frac{B(q)}{F(q)A(q)}u(k) + \frac{C(q)}{D(q)A(q)}v(k) \tag{6}$$

Considering q^{-1} as the time delay operator, then $y(k)q^{-1} = y(k - 1)$, $v(k)$ represents the noise, e $A(q)$, $B(q)$, $C(q)$, $D(q)$, $F(q)$ represent polynomials functions defined as in Eqs. (7) and (11).

$$A(q) = 1 - a_1q^{-1} - \dots - a_{ny}q^{-ny} \tag{7}$$

$$B(q) = 1 - b_1q^{-1} - \dots - b_{nu}q^{-nu} \tag{8}$$

$$C(q) = 1 - c_1q^{-1} - \dots - c_{nv}q^{-nv} \tag{9}$$

$$D(q) = 1 - d_1q^{-1} - \dots - d_{nd}q^{-nd} \tag{10}$$

$$F(q) = 1 - f_1q^{-1} - \dots - f_{nf}q^{-nf} \tag{11}$$

The general linear model representation can also be considered as

$$y(k) = G(q)u(k) + H(q)v(k) \tag{12}$$

In this representation, functions $G(q)$ and $H(q)$ are considered respectively process and noise functions, as shown in Fig. 2.

From the general linear model, several models can be derived with a few simplifications (Navrátil and Ivanka 2014). Two are particularly interesting, the ARX and the autoregressive model with moving average and exogenous inputs (ARMAX). The ARX model considers $C(q) = D(q) = F(q) = 1$ with $A(q)$ and $B(q)$ representing

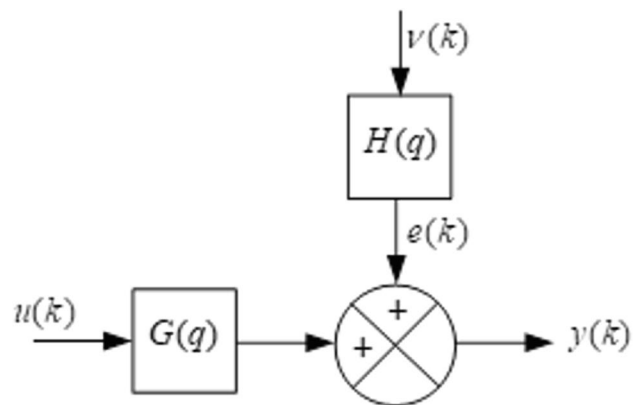


Fig. 2 General representation of estimated model

Table 2 Parameter for patients

Patient	Parameter					
	T (s)	$K0$	$K1$	b_{+0}	TAU (s)	MAPb (mmHg)
Type 1	25	0.3	0.001	0.0001	140	65
Type 2	30	0.4	0.0015	0.0001	140	65
Type 3	35	0.5	0.002	0.0001	150	65
Type 4	35	0.6	0.0025	0.0002	160	65
Type 5	40	0.7	0.0035	0.0002	170	65
Type 6	40	0.8	0.004	0.0002	180	65
Type 7	45	0.9	0.0045	0.0002	190	65
Type 8	45	1.0	0.005	0.0003	200	65
Type 9	50	1.1	0.0055	0.0003	210	65
Type 10	55	1.2	0.006	0.0003	220	65

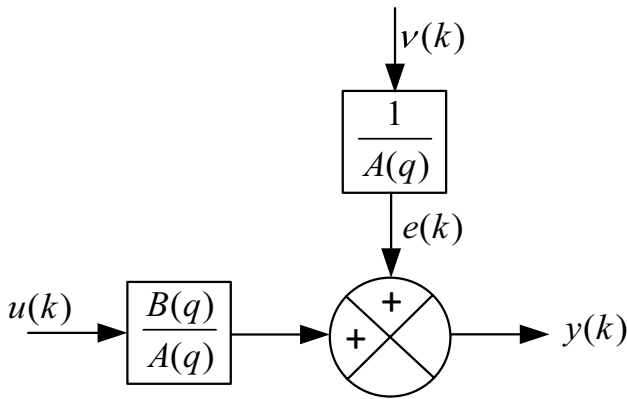


Fig. 3 ARX model representation

arbitrary polynomials to be estimated, resulting in the model according to Eq. (13) and Fig. 3.

$$y(k) = \frac{B(q)}{A(q)}u(k) + \frac{1}{A(q)}v(k) \tag{13}$$

From the ARX model, a linear differential equation can be obtained, relating the output to the inputs presented in Eq. (14) (Aruna and Jaya Christa 2020).

$$y(k) = a_1y(k - 1) + \dots + a_{na}y(k - n_a) + b_1u(k - 1) + \dots + b_{nb}u(k - n_b) + e(k) \tag{14}$$

From the ARX model, it is obtained θ defined as the system parameter vector and ϕ as the regressors vector.

$$\theta = [a_1 a_2 \dots a_{na} b_1 b_2 \dots b_{nb}]^T \tag{15}$$

$$\phi(k - 1) = [y(k - 1) \dots y(k - n_a) u(k - 1) \dots u(k - n_b)]^T \tag{16}$$

The ARMAX model assumes $D(q) = F(q) = 1$, and $A(q)$, $B(q)$, and $C(q)$ being the arbitrary polynomials to be estimated, resulting in the model according to Eq. (17) and Fig. 4.

$$y(k) = \frac{B(q)}{A(q)}u(k) + \frac{C(q)}{A(q)}v(k) \tag{17}$$

From ARMAX model a linear differential equation can be obtained, relating the output to the inputs, as shown in Eq. (18).

$$y(k) = a_1y(k - 1) + \dots + a_{na}y(k - n_a) + b_1u(k - 1) + \dots + b_{nu}u(k - n_u) + e(k) + c_1e(k - 1) + \dots + c_{nc}e(k - n_c) \tag{18}$$

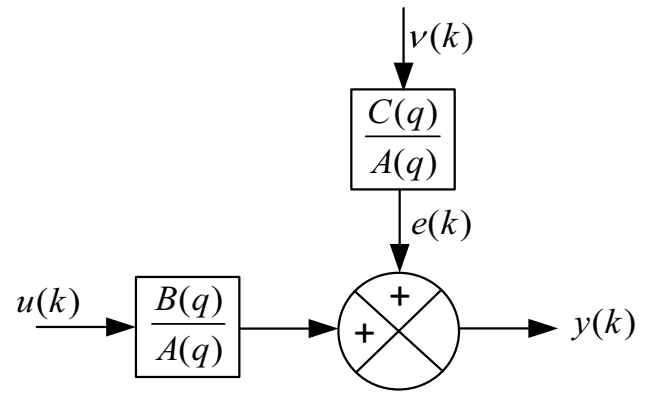


Fig. 4 ARMAX model representation

Therefore, from the ARMAX model we can obtain θ defined as the system parameter vector and ϕ as the regressors vector.

$$\theta = [a_1 a_2 \dots a_{na} b_1 b_2 \dots b_{nb} c_1 c_2 \dots c_{nc}]^T \tag{19}$$

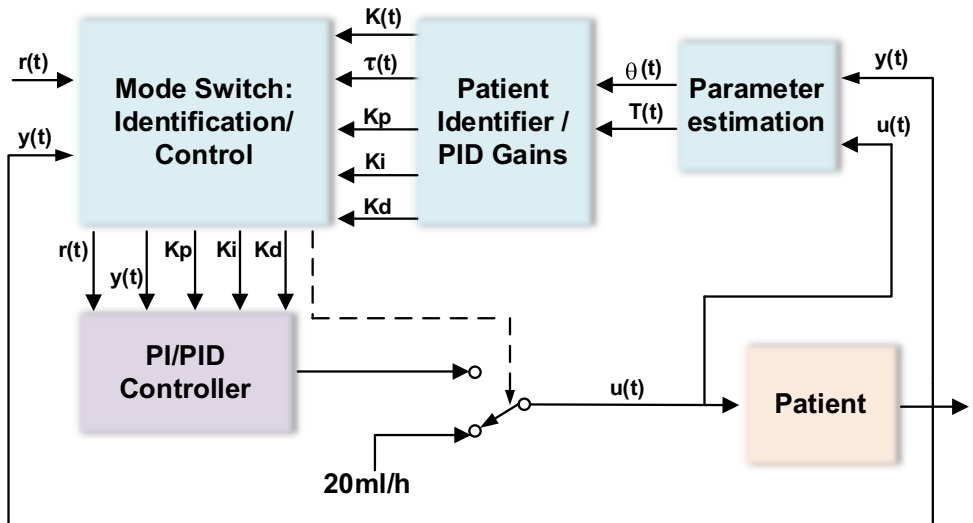
Adaptive PID controller design

The adaptive PID MAP controller (PID-AD) was designed to perform patient identification during a predefined time of 200 s, and after this identification period, the system works in automatic control mode. The identification time has taken into account the variability of all possible patients, from the least sensitive to the most sensitive. The block diagram proposed for this controller is shown in Fig. 5.

We calculated the PID-AD gains considering two criteria for performance comparison. The criteria adopted in this development are the control algorithm methods from the study by (Ziegler and Nichols 1942) in their PI (ZN-PI) and PID (ZN-PID) versions, and also the method (Skogestad 2004) known as Skogestad internal model control (SIMC).

In this work, the proposal for real-time estimation of patient parameters and calculation of controller gains is based on an ARX model used to describe the dynamics of the patient response.

Fig. 5 Block diagram of the proposed controller



The identification method used for the patient parameters is based on an ARX model estimator using a recursive least squares with forgetting factor estimation algorithm.

This estimator allows obtaining a discrete transfer function of the patient response, according to Eq. (14). Considering that the main transfer function of the MAP variation of the patient relative to the FNF infusion rate is a first-order function (Luspay and Grigoriadis 2015), then the model generated by the estimator is shown in Eq. (20).

$$G(z) = \frac{Y(z)}{U(z)} = \frac{b_0z^1 + b_1z^0}{a_0z^1 + a_1z^0} \tag{20}$$

And consequently, the estimated coefficients a_0 , a_1 , b_0 , and b_1 define the system response according to Eq. (21).

$$y(k) = \frac{B(q^{-1})}{A(q^{-1})}u(k) = \frac{b_0q^1 + b_1}{a_0q^1 + a_1}u(k) \tag{21}$$

The software implementation of the PID-AD controller is structured as shown in Fig. 6, using the polynomial recursive

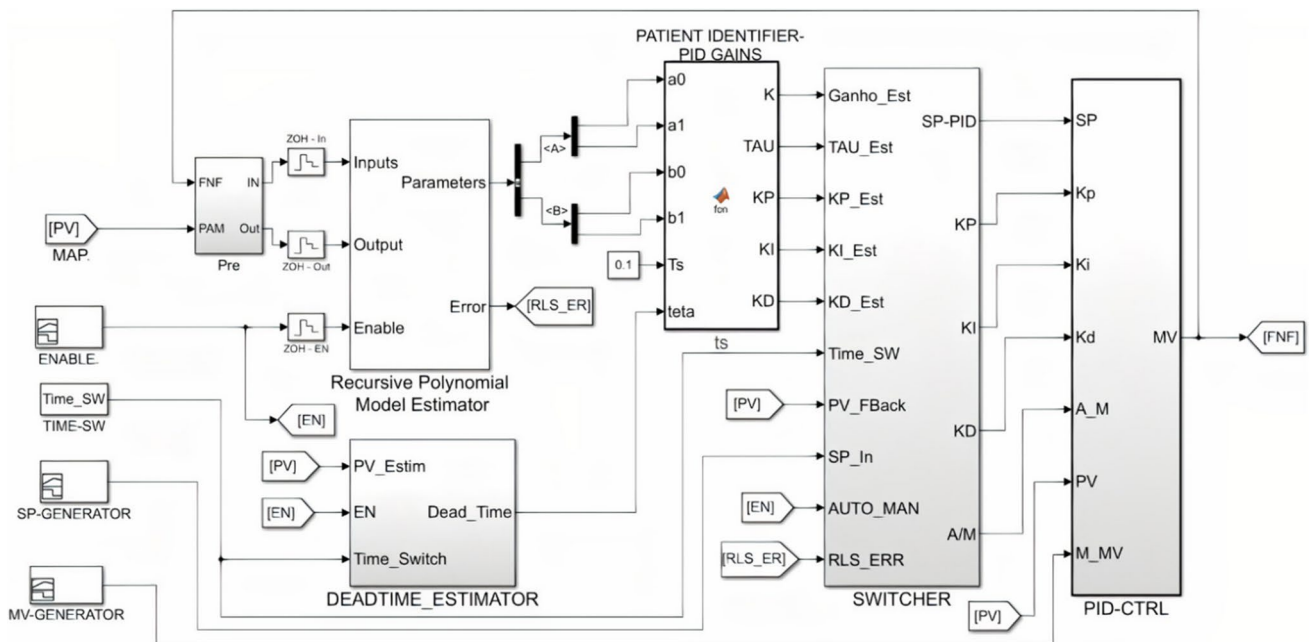


Fig. 6 Software implementation of PID-AD controller

model estimator block available in the MATLAB® libraries and its Simulink® module.

We developed the block for patient identification and PID gains to calculate the sensitivity, the delay time in the injection line, and the time constant of the drug application. The block also defines the values of the proportional gain (KP), integral gain (KI), and derivative gain (KD) of the controller. Equation (22) presents how the sensitivity is calculated. Equation (23) defines the time constant of drug application corresponding to drug absorption, distribution, and metabolism.

$$K = \frac{(b0 + b1)}{(a0 + a1)} \tag{22}$$

$$\tau = \frac{K}{(b1/Ts)} \tag{23}$$

The PID-CTRL block has one output tagged MV, corresponding to the PHP infusion rate. When the A_M input of the PID_CTRL block assumes a true status, defining that the PID is in automatic mode, the MV output is the result of the automatic calculation performed by the PID algorithm inside the block, as shown in Fig. 7. If the A_M input of the PID_CTRL block assumes a false state, defining that the PID is in manual mode, the MV output is a constant value.

In this study, the controller is in manual mode during the initial patient identification stage, with a fixed PHP rate of 20 mL/h provided by M_MV input. During this moment, a signal provided by the band-limited white noise block is added to the MV output signal of the PID-CTRL block. It generates a normally distributed random value, performing the persistent excitation function required for patient identification. Figure 7 shows these details inside the PID-CTRL control block.

In the block “recursive polynomial model estimator” shown in Fig. 6, the output error signal corresponds to the

estimation error signal. This signal is sufficiently low when the estimation achieves success. In this work, any value of this signal less than 0.00001 is considered a level of success in patient estimation. If during the 200 s for patient identification this error signal reaches a level equal to or below the setpoint, the controller assumes automatic control mode. Otherwise, the controller remains in the manual, ensuring the safe operation of the system in manual mode.

The estimation success condition check was implemented within the Switcher block, shown in Fig. 6. This estimation failure status can be observed during system operation by warnings on a screen of the supervisory system integrated with the controller through the existing communication between controller and supervisory. Figure 10 shows the supervisory screen of this system.

The system set the controller gain for each identified patient case. To achieve the best performance, in this work, we used three heavily used methods for tuning gains in control systems, ZN-PI, ZN-PID, and SIMC control algorithms. Table 3 presents the equations relative to the three methods.

We designed the switch block so that after the determined time for patient parameter identification, called the switching time, the patient parameter identification mode and the system control mode are switched automatically. At the instant that mode transfer is performed, the block responsible for patient identification and PID gains transfers the current values to the PID controller, which from that moment on uses

Table 3 PID gains forms

Control type	Gains		
	KP	KI	KD
ZN PI	$Kp = \frac{0.9 \times \tau}{(T \times K)}$	$Ki = \frac{0.3}{T}$	0
ZN PID	$Kp = \frac{1.2 \times \tau}{(T \times K)}$	$Ki = \frac{1}{2 \times T}$	$Kd = 0.5 \times T$
SIMC	$Kp = \frac{\tau}{K \times (\tau/2 + T)}$	$Ki = \frac{1}{\tau}$	0

Fig. 7 Details of band-limited white noise block for persistent excitation

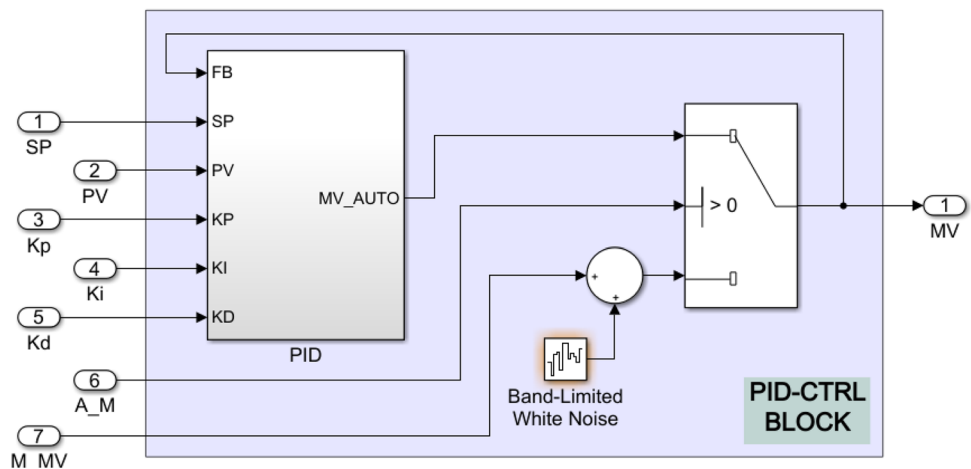
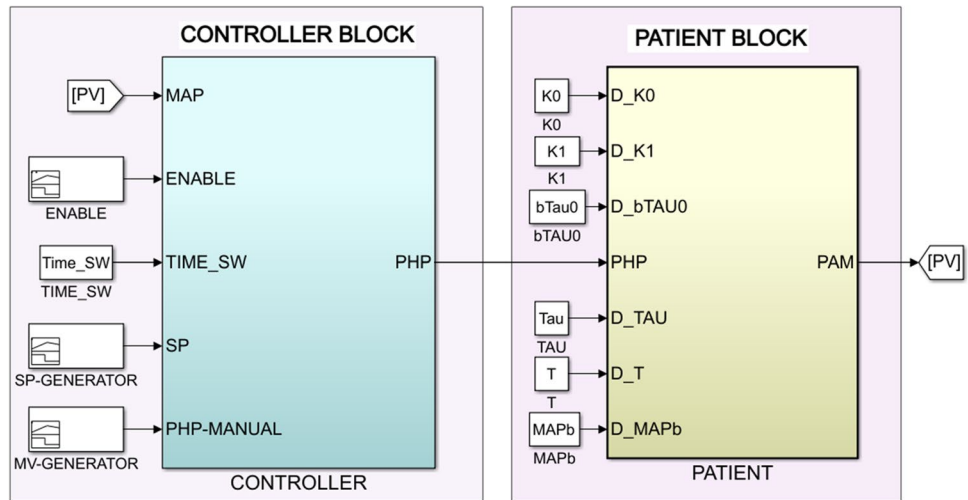


Fig. 8 System architecture for adaptive PID controller software simulation



them as parameters for the control. The PID control output set the PHP infusion rate in the control mode.

We performed the model implementation in a Windows PC i7 Desktop computer with 8 Gb of RAM with support from MATLAB/Simulink® (v. 2019a, license number 40686582). As shown in Fig. 8, the architecture of the computer simulation system has two blocks, the patient simulation unit and the adaptive PID controller block. Both were assembled in MATLAB/Simulink.

Hardware implementation

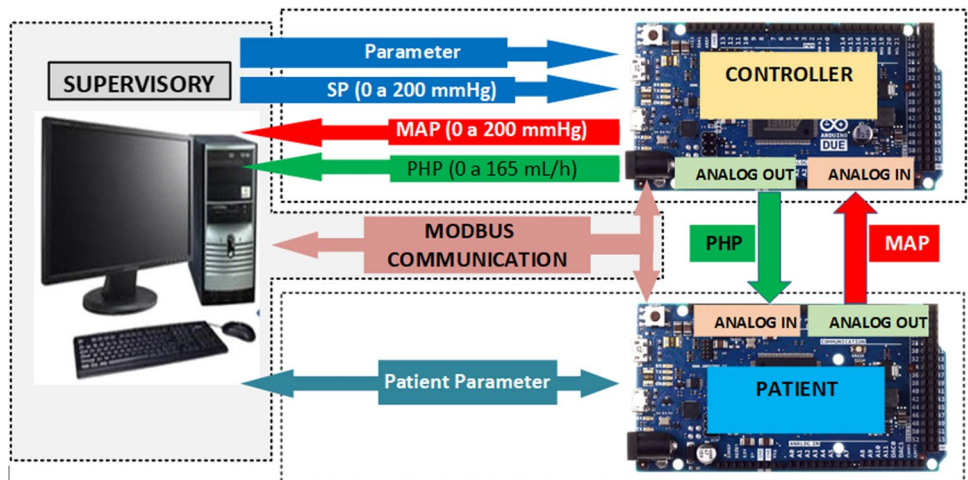
The evaluation of the controller was performed using a real-time hardware-in-the-loop (HIL) simulation and compared to the software simulation. The hardware implementation to evaluate the system performance was embedded on two Arduino DUE boards with a 32-bit ARM Cortex-M3 Atmel SAM3X8E microcontroller, 512 Kb of Flash memory, 12-bit analog to digital converter, and 12-bit digital to analog converter. One of the boards simulates the dynamics of the

patient in real-time while the other performs the controller functions, according to the architecture shown in Fig. 9. The algorithm was initially obtained by the MATLAB/Simulink® code generator using C++ language from the software simulation. After this step, we treated the algorithm for the hardware board in the specific interface device environment program (IDE).

We configured several parameters as constants during the software simulation. These parameters are configured in the hardware simulation from a supervisory system, as shown in Fig. 10. In hardware simulation, it allows adjusting the reference value of MAP, the initial value of the PHP infusion rate at any time. We designed the supervisory system using the free educational version of the Indusoft Web Studio software. The supervisory system communicates with the hardware through the MODBUS protocol at a rate of 1 sample every 0.5 s. This system collects and stores all data produced during the simulation.

The test procedure consists of the MAP response analysis considering two main phases: patient identification and

Fig. 9 Hardware implementation of PID-AD controller



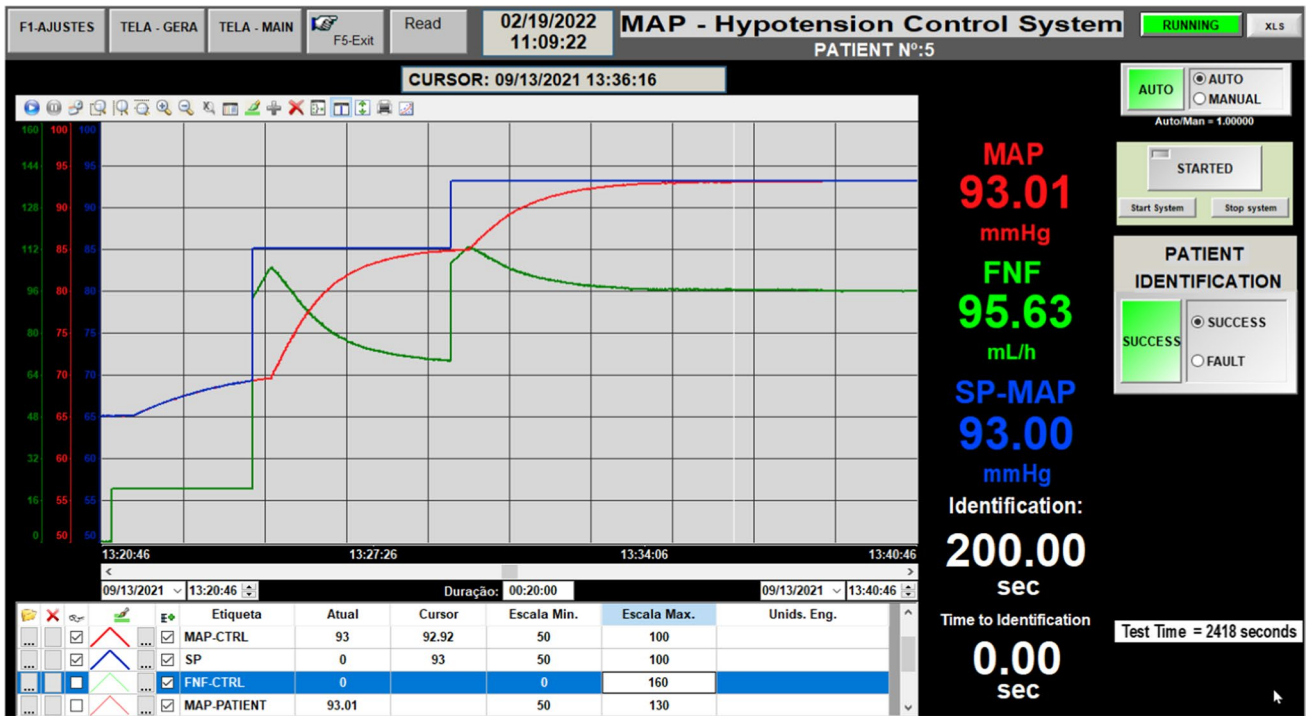


Fig. 10 Supervisory system for MAP PID-AD controller

effective control. In the identification phase, the system injects PHP with a fixed rate of 20 ml/h during the first 200 s. After this phase, the system switches to the control phase, consisting of two stages. In the first stage, the PID-AD controller assumes the drug injection automatically. The PID-AD controller sets the SP value of MAP at 85 mmHg during 300 s. In the second stage, the SP changes to 93 mmHg maintaining this value for next 630 s. Therefore, the performance analysis of the controller occurred during the 930 s after the initial 200 s of identification, totalizing 1130 s of the test.

Results

Frequently, automatic MAP controllers are evaluated with patient parameters changing into three types: insensitive, nominal, and sensitive (Silva et al. 2019). In this study, we tested the control for ten different types of patients, according to Table 2. Tables 4, 5, and 6 present the values obtained for gain, time constant, and dead time of the patient response, calculated from Eqs. (22) and (23), and the controller gains KP, KI, and KD calculated by the equations in Table 3, immediately after the 200 s corresponding to the patient identification step. We collected the results in

Table 4 Software and hardware simulation data for ZN-PI

Pat. type	KP		KI		Gain		Tau		Teta	
	SW	HW	SW	HW	SW	HW	SW	HW	SW	HW
1	12.53	12.545	0.008696	0.008280	0.299	0.312	143.7	157.55	34.5	35.2
2	8.891	8.803	0.008174	0.008350	0.4002	0.393	145.1	138.28	36.7	35.9
3	7.058	6.804	0.007538	0.007370	0.5017	0.495	156.6	152.33	39.8	40.7
4	6.319	6.108	0.007595	0.007480	0.6011	0.589	166.7	160.46	39.5	40.1
5	5.308	5.175	0.006977	0.006810	0.7005	0.708	177.7	179.3	43.0	44.0
6	4.924	4.783	0.006993	0.007000	0.7981	0.796	187.3	181.17	42.9	42.8
7	4.276	4.266	0.006438	0.006420	0.9025	0.941	199.8	208.33	46.6	46.7
8	4.058	3.949	0.006452	0.006220	0.9992	1.024	209.5	216.74	46.5	48.2
9	3.582	3.532	0.005929	0.005790	1.108	1.149	223.1	233.65	50.6	51.8
10	3.189	3.165	0.005455	0.005410	1.223	1.244	238.3	242.55	55	55.4

Table 5 Software and hardware simulation data for ZN-PID

Pat. type	KP		KI		KD		Gain		Tau		Teta	
	SW	HW	SW	HW	SW	HW	SW	HW	SW	HW	SW	HW
1	16.71	16.966	0.01449	0.014120	17.25	17.7	0.299	0.310	143.7	155.36	34.5	35.4
2	11.85	11.425	0.01362	0.013190	18.35	18.95	0.4002	0.400	145.1	144.57	36.7	37.5
3	9.41	9.328	0.01256	0.012340	19.9	20.25	0.5017	0.518	156.6	163.10	39.8	40.5
4	8.426	8.224	0.01266	0.012130	19.75	20.6	0.6011	0.621	166.7	175.00	39.5	41.2
5	7.078	6.800	0.01163	0.011330	21.5	22.05	0.7005	0.711	177.7	177.71	43.0	44.1
6	6.565	6.419	0.01166	0.01126	21.45	22.2	0.7981	0.826	187.3	196.21	42.9	44.4
7	5.701	5.533	0.01073	0.010413	23.3	23.95	0.9025	0.931	199.8	205.85	46.6	47.9
8	5.41	5.196	0.01075	0.010460	23.25	23.90	0.9992	0.986	209.5	204.28	46.5	47.8
9	4.776	4.662	0.009881	0.009610	25.3	26.00	1.108	1.122	223.1	226.71	50.6	52.0
10	4.251	4.213	0.009091	0.009040	27.5	27.65	1.223	1.234	238.3	239.76	55.0	55.3

Table 6 Software and hardware simulation data for SIMC

Pat. type	KP		KI		Gain		Tau		Teta	
	SW	HW	SW	HW	SW	HW	SW	HW	SW	HW
1	4.519	4.616	0.006961	0.007020	0.299	0.300	143.7	142.38	34.5	31.4
2	3.319	3.350	0.006893	0.006820	0.4002	0.406	154.1	146.54	36.7	34.9
3	2.643	2.606	0.006386	0.006150	0.5017	0.515	156.6	162.35	39.8	39.6
4	2.258	2.265	0.005999	0.005940	0.6011	0.611	166.7	168.17	39.5	37.6
5	1.924	1.880	0.005629	0.005380	0.7005	0.727	177.7	185.81	43.0	43.0
6	1.719	1.707	0.005339	0.005210	0.7981	0.816	187.3	191.73	42.9	41.6
7	1.511	1.481	0.005005	0.004800	0.9025	0.927	199.8	207.99	46.6	47.4
8	1.386	1.380	0.004774	0.004930	0.9992	0.984	209.5	202.81	46.5	47.8
9	1.242	1.272	0.004482	0.005180	1.108	1.019	223.10	192.68	50.6	52.2
10	1.119	1.091	0.004196	0.003990	1.223	1.272	238.30	250.12	55.0	55.0

Table 7 Hardware performance results

Pat. type	SSE (mmHg)			OS (mmHg)			ST (s)		
	SIMC	ZNPI	ZNPID	SIMC	ZNPI	ZNPID	SIMC	ZNPI	ZNPID
1	0.01	0.02	0.04	0.06	0.09	0.93	143.5	57.5	62.5
2	-0.09	-0.01	-0.02	-0.02	2.17	1.97	149.5	126.0	126.0
3	-0.12	-0.09	-0.04	-0.11	2.31	4.58	166.0	165.0	144.5
4	-0.04	-0.04	0.04	0.00	2.66	3.90	163.5	204.5	150.5
5	-0.12	-0.04	0.09	-0.12	2.84	5.21	175.5	186.5	166.0
6	-0.17	-0.03	0.07	-0.10	3.11	5.30	171.5	184.0	169.5
7	-0.13	-0.02	-0.19	-0.19	3.63	5.53	172.5	154.5	191.0
8	-0.06	0.04	-0.23	0.00	3.58	5.53	165.0	159.0	194.5
9	-0.08	-0.09	0.04	-0.05	4.34	5.37	168.5	163.5	216.0
10	-0.07	-0.14	0.31	0.01	4.34	5.21	166.5	235.0	240.5

software and hardware simulation after the patient identification stage for an adaptive control system based on the ZN-PI, ZN-PID, and SIMC methods.

Figure 11 shows the MAP control response for type 1, 5, and 10 patients. This figure allows the comparison results of the computer simulation, with the architecture is already shown in Fig. 7, and the simulation of the embedded HIL model with

architecture already shown in Fig. 8. The comparison shows the control phase, exactly after the initial 200 s used for patient identification. In the simulation, it is possible to verify that the steady-state error (SSE) was less than 0.21 mmHg for SIMC

Fig. 11 MAP control response: **a** Patient 01, **b** Patient 05 and **c** Patient 10

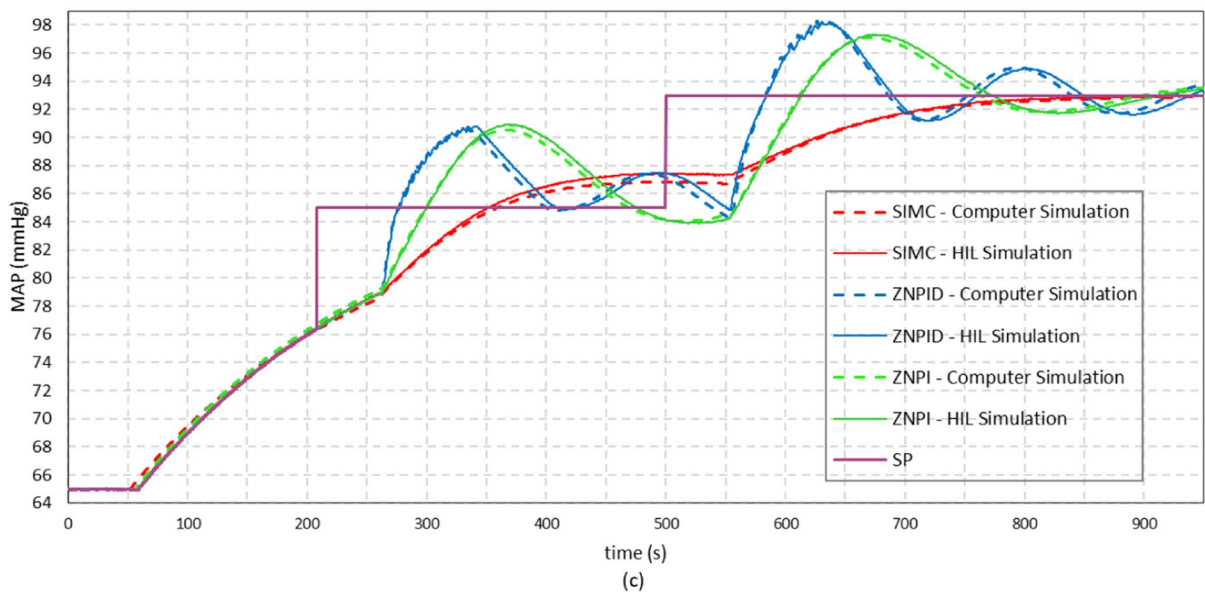
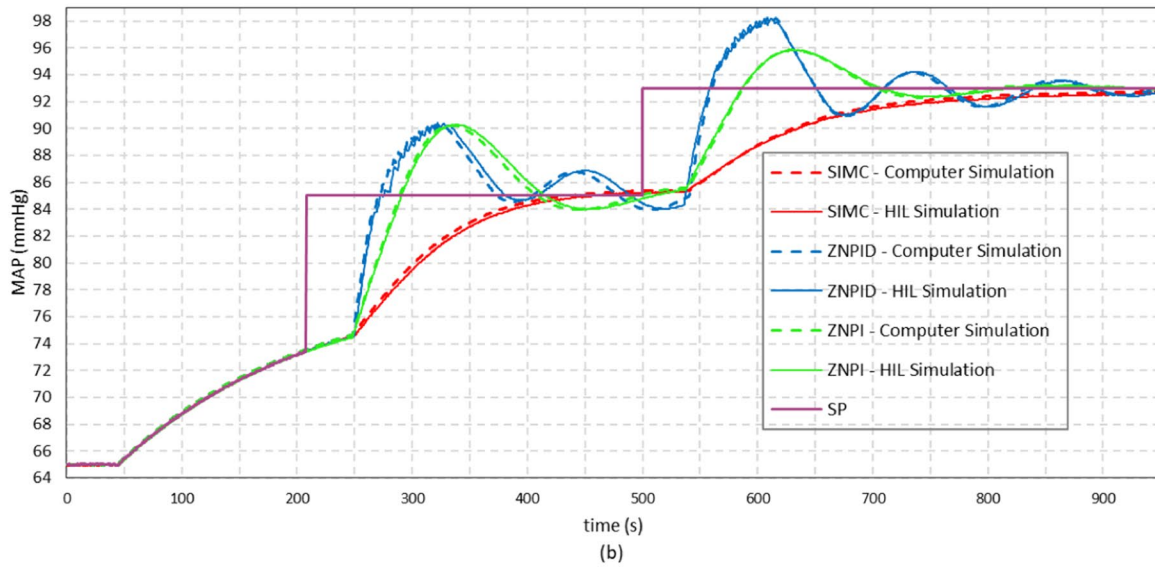
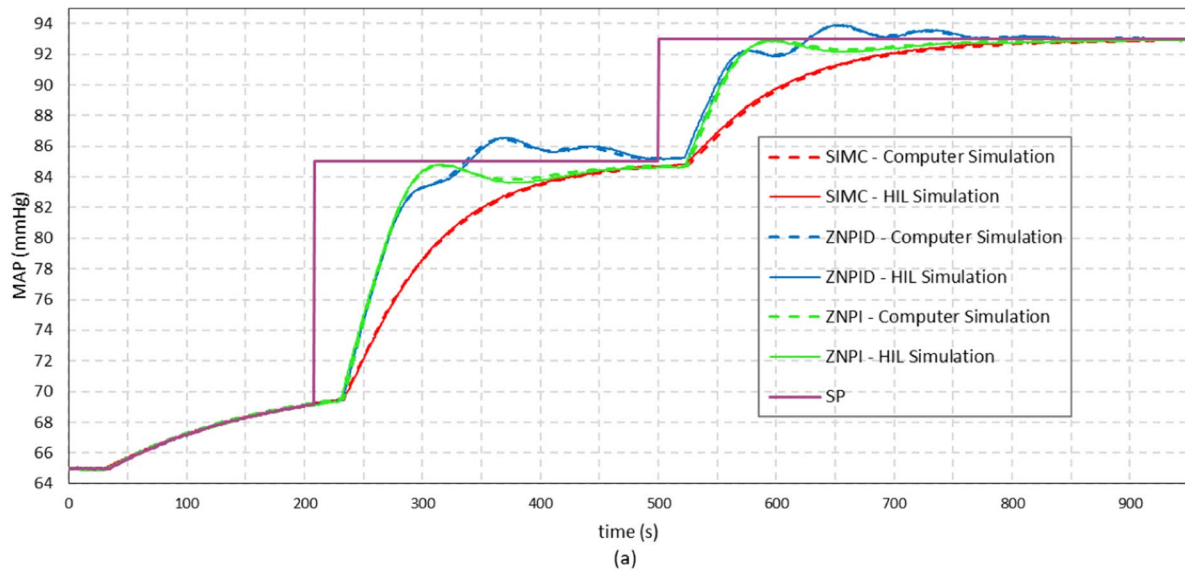


Table 8 Controller performance results for the patient in full range

Control type	SSE (mmHg)	OS (mmHg)	ST (s)	IAE	ISE
	min ~ max	max	min ~ max	min ~ max	min ~ max
SIMC	− 0.01 ~ − 0.13	0.06	143.5 ~ 175.5	1725.7 ~ 2401.3	7482.6 ~ 19,652.0
ZN-PI	− 0.01 ~ 0.14	4.34	57.5 ~ 235.0	1459.7 ~ 2311.2	10,100.0 ~ 12,961.0
ZN-PID	− 0.02 ~ 0.31	5.53	62.5 ~ 240.5	1483.9 ~ 2094.4	9805.8 ~ 12,756.0
Performance criteria	± 5.0	5.8	270		

control, less than 0.31 mmHg for ZN-PID control, and less than 0.14 mmHg for ZN-PI control. The system achieved the desired MAP value of 93 mmHg with an overshoot value (OS) less than 0.06 mmHg for SIMC control, less than 5.53 mmHg for ZN-PID control and less than 4.34 mmHg for ZN-PI control. The settling time (ST) variation was from 143.5 to 175.5 s for the SIMC control, from 57.5 to 235 s for the ZN-PID control, and between 62.5 and 240.5 s for the ZN-PI control, according to Table 7.

Discussion

We analyzed the controller performance in the three gain settings proposals for the PID algorithm, based on the ZN-PI, ZN-PID, and SIMC criteria. The analysis was carried out using the criteria defined as SSE, ST, OS, the absolute error integral (IAE) and the squared error integral (ISE), as shown in Table 8. The table shows the minimum and maximum simulation parameters performed on all ten patient types.

We compared the values obtained in the three controllers' tests using performance criteria established by Luspay and Grigoriadis (2015). All three controllers showed a successful result, but the performance of the SIMC control type is particularly interesting, because of the low values for the OS and ST indexes, allowing a smoother control of the MAP control.

Despite the maximum IAE and ISE of the SIMC control type being higher than other control types, in 6 of the 10 simulated patients, these values were lower, which denotes SIMC performance was not worse compared to the other control types.

The proposed MAP PID-AD controller shows feasibility for implementation in clinical applications and aggregates value because it is a low-cost device and simple hardware. In this work, we did perform animal studies or human clinical trials. Therefore, more researches in future studies are required to test and validate the controller in an ideal environment and a full range of variations.

Conclusion

This paper presents the development of two devices, first to simulate different patients and the other for MAP regulation. A simple physiological model expressed by a first-order

function with varying parameters was used to characterize the MAP response as a function of PHP drug infusion, allowing the simulation of the patient's response. The named PID-AD controller is a simple and low-cost alternative to identify and control the MAP for several types of patients in a hypotensive situation. PID-AD processes a real-time estimation of the pharmacological response of patients and utilizes this information to calculate in the control algorithm. The MAP regulation results achieved here suggest that the PID-AD, compared to other reference work in the literature is a simple, non-complex tool for controlling hypotension, showing feasibility for use in perioperative and intensive care units.

Acknowledgements The research was supported by the University of Mogi das Cruzes–UMC and São Paulo Research Foundation – FAPESP through project no. 2017/16292-1

Declarations

Ethics approval and consent to participate This study does not involve the use of animal or human tests, only computational simulations were performed.

Conflict of interests The authors declare that they have no conflict of interest.

References

- Aguirre LA. Introdução à Identificação de Sistemas: técnicas lineares e não-lineares: teoria e aplicação, 4. ed. rev. 2015. Belo Horizonte
- Aruna R, Jaya Christa ST. Modeling, system identification and design of fuzzy PID controller for discharge dynamics of metal hydride hydrogen storage bed. *Int J Hydrogen Energy*. 2020;45:4703–19. <https://doi.org/10.1016/j.ijhydene.2019.11.238>.
- Coelho MS, Silva SJ, Boschi SRMS, et al. Real-time simulation device for mean arterial pressure of hypotensive patient subjected phenylephrine infusion. *Electron Lett*. 2020;56:865–8. <https://doi.org/10.1049/el.2020.1383>.
- da Silva SJ, Scardovelli TA, Boschi SR, et al. Simple adaptive PI controller development and evaluation for mean arterial pressure regulation. *Res Biomed Eng*. 2019;35:157–65. <https://doi.org/10.1007/s42600-019-00017-y>.
- das Neves JFNP, Monteiro GA, de Almeida JR, et al. Phenylephrine for blood pressure control in elective cesarean section: therapeutic versus prophylactic doses. *Brazilian J Anesthesiol*. 2010;60:391–8. [https://doi.org/10.1016/s0034-7094\(10\)70048-9](https://doi.org/10.1016/s0034-7094(10)70048-9).

- Davoud S, Gao W, Riveros-Perez E. Adaptive optimal target controlled infusion algorithm to prevent hypotension associated with labor epidural: an adaptive dynamic programming approach. *ISA Trans.* 2020;100:74–81. <https://doi.org/10.1016/j.isatra.2019.11.017>.
- De Carvalho A, Justo JF, Angelico BA, et al. Rotary inverted pendulum identification for control by paraconsistent neural network. *IEEE Access.* 2021;9:74155–67. <https://doi.org/10.1109/ACCESS.2021.3080176>.
- Fung P, Dumont G, Ansermino M, et al. Toward an advisory system for cesarean section spinal anesthesia. In: *Proceedings of the American Control Conference*. Institute of Electrical and Electronics Engineers Inc. 2004. pp 952–957
- Huang JW, Roy RJ. Multiple-drug hemodynamic control using fuzzy decision theory. *IEEE Trans Biomed Eng.* 1998;45:213–28. <https://doi.org/10.1109/10.661269>.
- Kashihara K, Kawada T, Uemura K, et al. Adaptive predictive control of arterial blood pressure based on a neural network during acute hypotension. *Ann Biomed Eng.* 2004;32:1365–83. <https://doi.org/10.1114/B:ABME.0000042225.19806.34>.
- Kashihara K. Automated drug infusion system based on deep convolutional neural networks. In: *Proceedings - 2018 IEEE International Conference on Systems, Man, and Cybernetics, SMC 2018*. 2018. Institute of Electrical and Electronics Engineers Inc., pp 1653–1657
- Lee JE, George RB, Habib AS. Spinal-induced hypotension: incidence, mechanisms, prophylaxis, and management: summarizing 20 years of research. *Best Pract Res Clin Anaesthesiol.* 2017;31:57–68. <https://doi.org/10.1016/j.bpa.2017.01.001>.
- Luspay T, Grigoriadis K. Robust linear parameter-varying control of blood pressure using vasoactive drugs. *Int J Control.* 2015;88:2013–29. <https://doi.org/10.1080/00207179.2015.1027953>.
- Monk TG, Bronsert MR, Henderson WG, et al. Association between intraoperative hypotension and hypertension and 30-day postoperative mortality in noncardiac surgery. *Anesthesiology.* 2015;123:307–19. <https://doi.org/10.1097/ALN.0000000000000756>.
- Navrátil P, Ivanka J. Recursive estimation algorithms in Matlab & Simulink development environment. *WSEAS Trans Comput.* 2014;13:691–702.
- Ngan Kee WD, Tam YH, Khaw KS, et al. Closed-loop feedback computer-controlled infusion of phenylephrine for maintaining blood pressure during spinal anaesthesia for caesarean section: A preliminary descriptive study. *Anaesthesia.* 2007;62:1251–6. <https://doi.org/10.1111/j.1365-2044.2007.05257.x>.
- Ngan Kee WD, Khaw KS, Ng FF, Tam YH. Randomized comparison of closed-loop feedback computer-controlled with manual-controlled infusion of phenylephrine for maintaining arterial pressure during spinal anaesthesia for Caesarean delivery. *Br J Anaesth.* 2012;110:59–65. <https://doi.org/10.1093/bja/aes339>.
- Ngan Kee WD, Khaw KS, Tam YH, et al. Performance of a closed-loop feedback computer-controlled infusion system for maintaining blood pressure during spinal anaesthesia for caesarean section: a randomized controlled comparison of norepinephrine versus phenylephrine. *J Clin Monit Comput.* 2017;31:617–23. <https://doi.org/10.1007/s10877-016-9883-z>.
- Rhodes A, Evans LE, Alhazzani W, et al. *Surviving Sepsis Campaign: International Guidelines for Management of Sepsis and Septic Shock*: 2016. *Intensive Care Med.* 2017;43:304–77. <https://doi.org/10.1007/s00134-017-4683-6>.
- Rinehart J, Alexander B, Manach YL, et al. Evaluation of a novel closed-loop fluid-administration system based on dynamic predictors of fluid responsiveness: An in silico simulation study. *Crit Care.* 2011;15. <https://doi.org/10.1186/cc10562>
- Rinehart J, Ma M, Calderon MD, Cannesson M. Feasibility of automated titration of vasopressor infusions using a novel closed-loop controller. *J Clin Monit Comput.* 2017;32:5–11. <https://doi.org/10.1007/s10877-017-9981-6>.
- Rinehart J, Lee S, Saugel B, Joosten A. Automated Blood Pressure Control. *Semin Respir Crit Care Med.* 2021;42:47–58. <https://doi.org/10.1055/s-0040-1713083>.
- Rinehart J, Joosten A, Ma M, et al. Closed-loop vasopressor control: in-silico study of robustness against pharmacodynamic variability. *J Clin Monit Comput.* 2018
- Sathish D, Nachiappan A. Automatic drug delivery system for the drug adrenaline using Pi, Pid, Imc & Mpc controllers. *Int J Recent Technol Eng.* 2019;7:2043–7.
- Skogestad S. Simple analytic rules for model reduction and PID controller tuning. *Model Identif Control.* 2004;25:85–120. <https://doi.org/10.4173/mic.2004.2.2>.
- Slate JB, Sheppard LC. Automatic control of blood pressure by drug infusion. *IEE Proc A Phys Sci Meas Instrumentation Manag Educ Rev.* 1982;129:639–45. <https://doi.org/10.1049/ip-a-1.1982.0101>.
- Soltész K, Sturk C, Paskevicius A, et al. Closed-loop prevention of hypotension in the heartbeating brain-dead porcine model. *IEEE Trans Biomed Eng.* 2017;64:1310–7. <https://doi.org/10.1109/TBME.2016.2602228>.
- Sun LY, Wijeyesundera DN, Tait GA, Beattie WS. Association of intraoperative hypotension with acute kidney injury after elective noncardiac surgery. *Anesthesiology.* 2015;123:515–23. <https://doi.org/10.1097/ALN.0000000000000765>.
- Tasoujian S, Salavati S, Franchek M, Grigoriadis K. Robust IMC-PID and parameter-varying control strategies for automated blood pressure regulation. *Int J Control Autom Syst.* 2019;17:1803–13. <https://doi.org/10.1007/s12555-018-0631-7>.
- Tasoujian S, Salavati S, Franchek MA, Grigoriadis KM. Robust delay-dependent LPV synthesis for blood pressure control with real-time Bayesian parameter estimation. *IET Control Theory Appl.* 2020;14:1334–45. <https://doi.org/10.1049/iet-cta.2019.0651>.
- Van Waes JAR, Van Klei WA, Wijeyesundera DN, et al. Association between intraoperative hypotension and myocardial injury after vascular surgery. *Anesthesiology.* 2016;124:35–44. <https://doi.org/10.1097/ALN.0000000000000922>.
- Wassar T, Luspay T, Upendar KR, et al. Automatic control of arterial pressure for hypotensive patients using phenylephrine. *Int J Model Simul.* 2014;34:187–98. <https://doi.org/10.2316/Journal.205.2014.4.205-6087>.
- Wesselink EM, Kappen TH, Torn HM, et al. Intraoperative hypotension and the risk of postoperative adverse outcomes: a systematic review. *Br J Anaesth.* 2018;121:706–21. <https://doi.org/10.1016/j.bja.2018.04.036>.
- Ziegler JG, Nichols NB. Optimum settings for automatic controllers. *Trans ASME.* 1942;64:759–68.

Publisher's Note Springer Nature remains neutral with regard to jurisdictional claims in published maps and institutional affiliations.